Self-Isolation and Testing Behaviour During the COVID-19 Pandemic: An Agent-Based Model

Umberto Gostoli*
University of Glasgow
  MRC/CSO Social and
    Public Health Sciences Unit
  umberto.gostoli@glasgow.ac.uk

Eric Silverman
University of Glasgow
  MRC/CSO Social and
    Public Health Sciences Unit

Abstract   Since the beginning of the COVID-19 pandemic, various models of virus spread have been proposed. While most of these models focused on the replication of the interaction processes through which the virus is passed on from infected agents to susceptible ones, less effort has been devoted to the process through which agents modify their behaviour as they adapt to the risks posed by the pandemic. Understanding the way agents respond to COVID-19 spread is important, as this behavioural response affects the dynamics of virus spread by modifying interaction patterns. In this article, we present an agent-based model that includes a behavioural module determining agent testing and isolation propensity in order to understand the role of various behavioural parameters in the spread of COVID-19.

1   Introduction

Following its appearance in late 2019, the SARS-CoV-2 virus or COVID-19 has become the most significant global pandemic since the 1918 influenza pandemic. By 15 March 2022 the World Health Organization recorded over 456 million confirmed COVID-19 cases worldwide, and over 6.04 million deaths (https://covid19.who.int/). Excess mortality estimates place the global death toll between January 2020 and December 2021 at 18.2 million (Wang et al., 2022). The scale and severity of this global crisis, and the subsequent need for severe public health restrictions to be implemented worldwide, has generated significant interest in using agent-based models (ABMs) to simulate the spread of the pandemic and its effects.

ABMs enable modellers to examine the impact of individual behaviour on population-level outcomes, and in the context of the global pandemic, this approach has been used to examine how individual behaviour influences the capacity for various interventions to reduce the spread of COVID-19. For example, Rajabi et al. (2021) have investigated the impact of social distancing restrictions and travel restrictions on COVID-19 spread; Koehler et al. (2021) have developed an ABM designed to assist policy-makers in making decisions on lifting pandemic restrictions; and Almagor and Picascia (2020) have investigated the efficacy of contact-tracing apps in containing the spread of the virus. While the use of ABMs has proliferated during the COVID-19 crisis, the question of how ABMs can be used most effectively remains a focus of significant debate: See, for

---

 * Corresponding author.

example, Dignum (2021), the subsequent review (Chattoe-Brown, 2021), and numerous comments at https://rofasss.org/tag/jasss-covid19-thread/.

Building simulation models of the pandemic and its effects requires an understanding of human behavioural responses to the spread of the virus in their community. Born et al.'s (2021) empirical study indicates that people do respond to the risk imposed by a pandemic by reducing their mobility. Using data from Google COVID-19 Community Mobility Reports (https://www.google.com/covid19/mobility/) for Sweden (a country where compulsory lockdowns have not been imposed), this work shows that the mobility of the population decreased considerably during the first wave of the pandemic, although significantly less than in countries where lockdown policies were implemented. Other empirical studies shed some light on the factors affecting self-isolation and adherence to lockdown policies. Smith et al. (2020), in their study of factors associated with self-isolation in the United Kingdom, found evidence that self-isolation increases with increased worry about COVID-19 and increased perceived likelihood of catching the virus. Moreover, they found that self-isolation is affected by the perceived social norm and by the help received from someone outside the household. Pullano et al. (2020) found that, in France the reduced mobility after the lockdown was positively associated with the number of hospitalizations (which can be thought of as a proxy for the risk posed by the virus) and the socioeconomic conditions. Similarly, A. L. Wright et al. (2020), investigating the level of compliance with shelter-in-place policies in the United States, found that compliance with the policy increases with local income.

However, despite the widespread use of agent-based modelling, relatively few COVID-19 models have examined the impact of behavioural factors on how individuals respond to the risks posed by the pandemic. Instead, much of the extant modelling work is highly abstracted, and uses very simplified behavioural models. For example, Wilder et al. (2020) proposed an agent-based model in which out-of-household contacts are based simply on a country-specific contact matrix containing the mean number of daily contacts agents of an age group have with agents from each of the other age groups. Similarly, Silva et al. (2020) presented a model that allows agents to have differential exposure to risk according to their economic status, but does not include a facility for agents to modify their behaviour in accordance with their own perception of risk.

One of the first works accounting for the adaption of the behaviour of individuals during a pandemic was Epstein et al. (2008). Here, agents could be independently infected by the virus and by the *fear* of the virus. If infected by fear, agents self-isolate at a certain rate, until they recover from fear, ending their self-isolation. Shastry et al. (2022) have recently made progress in this area of COVID-19 modelling research by including a model of risk tolerance in an agent-based simulation of COVID-19 spread. In this model, agents have individual levels of risk tolerance, which is a decreasing function of age, and is adjusted towards the mean risk tolerance of groups with which they interact. The model focused on a U.S. policy context in which shelter-in-place orders were issued but were not legally enforceable; this meant that agents were able to freely defy the restrictions, if their risk tolerance allowed.

In this article, we present an agent-based model of COVID-19 spread that builds upon these foundations and includes a nuanced model of self-isolation behaviour. This behavioural module enables a feedback process, in which pandemic dynamics influence agent behaviour, which then influences pandemic dynamics in turn. The central contribution of this model is a behavioural module that allows households to reduce their social interaction as a response to the perceived risks posed by the virus; these risk perceptions are influenced by public information provided about the virus, the prevalence of COVID-19 infections within an agent's network of neighbours, and the tendency for their neighbours to self-isolate.

While the current model is a proof-of-concept, we propose that simulations including these behavioural elements may help policy-makers to design more effective interventions during future global health crises, including future waves of COVID-19 variants or other novel pathogens. Non-pharmaceutical interventions require compliance from the population in order to be maximally effective, and a deeper understanding of how public information and social context influence compliance may enable the development of more effective messaging.

2 General Framework

The simulation unfolds in two stages: In the first stage a demographic process proceeds in one-year steps, from year 1860 to year 2020, to create a population whose demographic and socioeconomic characteristics roughly replicate those of the U.K. population. In the second stage, the COVID-19 spread is simulated through one-day steps, starting at the beginning of the year 2020 for 360 days. In this article, we provide a brief summary of the demographic module, and refer the reader to Gostoli and Silverman (2019, 2020), Noble et al. (2012), and Silverman et al. (2013) for more details about this module (while the complete Python 2.7 source code for the simulation is available in our GitHub repository at https://github.com/UmbertoGostoli/Pandemic-Behaviour-Model/tree /Pandemic-Only-Sim).

We will describe in detail the novel modules introduced in this article, which are:

• the agent's social network;

• the virus exposure settings and processes;

• the behavioural module (defining isolation and testing behaviour); and

• the course of the virus.

2.1 Demographic Process

This stage begins with the generation of an initial population of couples, which are randomly distributed on a 8 × 12-cell grid approximating the geography of the United Kingdom. Each cell of the grid represents a town, and within each town a number of houses is created proportional to the U.K. population density. Each year, a series of demographic events drive the population's dynamics: births, marriages, divorces, and deaths. Empirical population data (in the form of U.K. Census data) is integrated into the model's demographic processes in 1951.

2.1.1 Agent Life Course

With a certain age-specific probability the couple's female will give birth. Agents enter adulthood at the working age of 16: At this point they can either start working or continue in education, a choice that is repeated at two-year intervals, until the age of 24.[1] After education, agents become employed, taking a salary that is a function of the education level they have reached (which is a stochastic function of their parents' socioeconomic status; see section 2.1.4). When agents reach retirement age (set at 65 in these simulations), they retire from employment. Mortality rates in the model follow Noble et al. (2012) and use a Gompertz-Makeham mortality model until 1951. From that point we use mortality rates drawn from the Human Mortality Database (https://www .mortality.org/). Lee-Carter projections generate agent mortality rates from 2009.

2.1.2 Partnership Formation and Dissolution

Once they reach working age, agents can form partnerships. Agents are paired randomly with probabilities that depend inversely on their age, geographical distance from one another, and socioeconomic differences. Age-specific annual divorce probabilities determine whether a couple dissolves their partnership in each year.

2.1.3 Internal Migration

Relocation happens most frequently due to agents finding a partner in a different town. Male agents relocate to new houses once a partnership dissolves, and any children produced by that partnership stay with the mother. Retired agents with care needs may move in with one of their adult children,

---

1 These two-year intervals represent educational stages corresponding roughly to U.K. education levels: A-level, Higher National Diploma, Degree, and Higher Degree.

with a probability determined by their care need level and the amount of care supply in their child's household. Orphaned children are adopted by a household in their kinship network, or by a random family if there are no available households in their kinship network. Apart from these specific, event-driven cases, households also relocate to another town with a certain probability that is inversely proportional to the relative cost of relocation, defined as the ratio between the total cost of relocation and the households' per capita income.

2.1.4 Socioeconomic Status and Income

Agents are placed in one of five socioeconomic status (SES) groups, based on the Approximated Social Grade from the Office for National Statistics (https://www.ukgeographics.co.uk/blog/social -grade-a-b-c1-c2-d-e). The model contains a *social mobility* process: An agent is assigned the SES group associated with the education level the agent has reached, with a probability of moving further up the education ladder depending on the household income and parental level of education. The introduction of SES groups has a number of effects on the various stages of the agent life course: A higher SES is associated with lower mortality and fertility rates, higher hourly salaries, and higher salary growth rate.

Every employed agent receives an hourly salary that is a function of the agent's SES and cumulative work experience. On the basis of the total income of the household's members, each household is assigned an *income quintile*, which affects a range of processes during the pandemic stage, such as the size of social networks, the probabilities to visit certain venues, the isolation propensities, and the probabilities to develop different conditions (see the next section for details).

2.1.5 Social Networks

Each agent is associated with a social network whose size is proportional to the total number of daily contacts associated with the agent's age and SES. These networks are created by randomly sampling agents from the population, and for each sampled agent, selecting a *friend* from the population with a probability that is proportional to:

- geographical distance,

- age difference,

- socioeconomic status' distance, and

- number of common friends.

Once a link is created between two agents, the probability of the link creation becomes the *weight* of that link, defining the importance of the relationship between the two agents. Formally, the weight of a connection, w_{ij}, is given by:

$$w_{ij} = \frac{1}{e^{\beta_n}} \tag{1}$$

where β_n is the sum of 4 elements: a function f of (a) the geographical distance, d; (b) the age difference, a; (c) the socioeconomic status' distance, s; and (d) the number of common friends, g. Formally, the four elements are given by the following equations:

$$f(d) = \alpha_d * d^{\beta_d} \tag{2}$$

$$f(a) = \alpha_a * a^{\beta_a} \tag{3}$$

$$f(s) = \alpha_s * s^{\beta_s} \tag{4}$$

$$f(g) = -\alpha_g * g^{\beta_g} \tag{5}$$

Parameter	Equation	Range	Default value
α_d	2–12	$[0, \infty]$	2.0
β_d	2–12	$[0, 1]$	0.001
α_a	3	$[0, \infty]$	2.0
β_a	3	$[0, 1]$	0.02
α_s	4–12	$[0, \infty]$	2.0
β_s	4–12	$[0, 1]$	0.2
α_g	5	$[0, \infty]$	0.5
β_g	5	$[0, 1]$	0.1

Figure 1. Social network parameters.

where the four α's and the four β's are parameters of the model. A summary of the parameters, together with their range and value used in the simulations presented in this article, is shown in Figure 1.

The process is repeated until, for each agent, a social network of the desired size has been created. These personal networks are associated with the networks connecting the households. Each household H is associated with:

- the households of the relatives of household H's members; and

- the households of the friends of household H's members.

The weights of the links between households are a function of the geographical distance between the households' towns.

The two networks have different roles in the information processing module through which agent behaviour is determined. While the personal friends network affects agent self-isolation propensity, *after this has been formed at a first, individual, level*, through agent tendency to adjust behaviour towards the mean of the network, the households network affects the formation of individual self-isolation propensity itself, by allowing agents to observe the occurrence of pandemic events and, therefore, providing them with the information they use to develop their subjective probabilities of these events.

2.2 The Interaction Processes

In the second stage, the COVID-19 spread is simulated from year 2020 for a period 360 days, through one-day time steps. We assume that, initially, the virus is brought into the U.K. from abroad by international travellers, a process that we will call *exogenous infection*. Then, the virus spreads within the U.K. by means of two main spreading mechanisms: *social interaction* and *within-household interaction*. We assume that the social interaction process depends on a household's decisions to isolate. After the incubation period, the infected individuals develop various conditions and, at the end of the infection period, either recover or die, as shown in Figure 2.

2.2.1 Exogenous Infections

In each period, a fixed share θ_e (which is a parameter of the model) of the adult, susceptible population is infected exogenously, i.e., through contacts they have with people from abroad. We assume that the probability of being part of this group, which can be thought as composed of international travellers, depends on an agent's socioeconomic status and the dimensions of the town they come from. Formally, the number of people becoming exposed through international travel, E_t, in each period is given by:

$$E_t = \theta_e S \qquad (6)$$

Parameter	Equation	Range	Default value
Exogenous infection			
θ_e	6	[0, 1]	0.0004
γ_e	7	[0, ∞]	0.1
Domestic infection			
ξ_h	9	[0, 1]	0.5
σ_h	9	[0, ∞]	0.5
β_h	10	[0, ∞]	0.05
Social infection			
ρ_s	11	[0, ∞]	1.0
δ_s	13	[0, ∞]	0.5
π_s	14	[0, ∞]	0.025

Figure 2. Parameters of the exposure processes.

where S is the number of susceptible agents. Then E_t agents are randomly sampled from the population of susceptible adults with probabilities proportional to the product of the functions of two agent-specific factors: a factor that depends on the agent's socioeconomic status, c, and the relative size of the agent's town (in terms of number of houses, t), where:

$$f(c) = e^{\gamma_e c} \qquad (7)$$

and

$$f(t) = \frac{t}{T} \qquad (8)$$

where T is the total number of houses, while γ_e is a parameter of the model.

2.2.2 Domestic Interaction

Domestic interaction infection is, together with infection through social interaction, part of the endogenous spread of the virus. We assume that the probability that a susceptible agent is infected by a member of its household is an increasing function of the number of infected household members and depends on knowledge of the infection (we assume that if an agent is knowingly infected, the household members will adopt prudential behaviour reducing the probability of transmission). More precisely, each agent is assigned a *viral load*, v, when it is exposed (randomly drawn from a uniform distribution), and we define the household's *infection risk factor*, r, as the ratio between the sum of the infected household members' viral loads and a function of the total number of infected agents. Formally:

$$r = \frac{\sum_{i=1}^{H} v_i d_h}{H^{\sigma_h}} \qquad (9)$$

where d_h is a dummy variable taking the value of 1 for agents who are unknowingly infectious and a value of $\xi_h < 1$ for agents who are knowingly infectious (the assumption being that if a household member is knowingly infectious, the other members will adopt a prudential behaviour reducing the probability of this agent transmitting the virus). H is the total number of household's members, and σ_h is a parameter of the model. The probability that an agent is infected within the domestic setting, p_h, is given by:

$$p_h = 1 - exp^{-\beta_h r} \qquad (10)$$

where β_h is a parameter of the model.

2.2.3   Social Interaction

In our model, social interaction takes place in a series of venues the agents attend. At the beginning of the pandemic stage, a number of venues is created in each town proportional to the town's population. In each day, we allocate agents to the venues in their town in a way that is consistent with the age-specific interaction matrix for the U.K., as estimated by Prem et al. (2017). Moreover, we assume that a certain percentage of agents visits other towns in each period, to account for daily intra-urban commuting.

Starting from empty venues, agents are sequentially allocated to venues in their town, with a probability that depends on:

- the geographical distance between an agent's house and the location of venues;
- the difference between the mean of the socioeconomic status of venue attendants and the socioeconomic status of the agents to be allocated (the assumption being that the choice of venues is partly driven by socioeconomic affinity); and
- the isolation rate of the agent.

In particular, the probability that an agent i is selected as an attendant of a venue j, is proportional to a factor q_v given by:

$$q_v = \frac{1}{exp^{\rho_v \chi}} \tag{11}$$

where ρ_v is a parameter of the model and χ is given by:

$$\chi = \alpha_s c^{\beta_s} + \alpha_d d^{\beta_d} \tag{12}$$

where c is the difference between the agent's socioeconomic status and the mean of the socioeconomic status of the venue attendants, d is the distance between the agent's house and the venue, and the two γ's and the two π's are four parameters of the model. Venues attendants are sampled randomly from the population, so in each period, an agent can visit more than one venue.

The probability of a susceptible agent attending a venue being infected is proportional to the number of infected agents attending that venue. More specifically, the number of contacts ν_s of each attending agent is determined by:

$$\nu_s = P^{\delta_v} \tag{13}$$

where P is the total number of venue attendants and δ_v is a parameter of the model (bounded between 0 and 1). Then, a set of P agents is randomly sampled from the set of venue attendants. The probability of an agent being infected by each of these sampled agents, p_s, is given by:

$$p_s = \pi_s v \tag{14}$$

where v is the viral load of the sampled agent (which is 0 if the agent is not infectious) and π_s is a parameter of the model. A table of the parameters of the exposure processes is shown in Figure 2.

2.3   The Behavioural Module

During the pandemic, the number of people attending venues decreases as people become aware that interaction with other people carries a risk of them getting the virus and, as a consequence,

they self-isolate. We assume that agent self-isolation rate is the result of an individual assessment of the risks and of social processes happening through their social network and their household membership.

As for the first, the individual element, the behavioral framework we introduce in this work is based on two cognitive processes: The first is the process through which agents discount probabilistic gains (and losses); the second is the process through which agents estimate probabilities of negative events. The two cognitive processes interact to determine the individually-determined agent self-isolation rate: First, agents estimate the probabilities of being infected and, if infected, of developing various conditions (i.e., being hospitalized, being intubated, or dying); then, with these probabilities agents compute the expected cost of unrestricted movement (which can be also considered the expected *gain* of self-isolation). We will consider the two modules in turn.

2.3.1 Expected Cost of Infection

Green et al. (1999) propose a hyperbolic function with two parameters to describe the discounted value of probabilistic gains (and losses), V. The function takes the following form:

$$V = \frac{C}{(1 + h\epsilon)^s} \tag{15}$$

with

$$\epsilon = \frac{1 - p^f}{p^f}$$

where p^f is the probability of infection when an agent does not isolate, and C represents the expected cost associated with infection, given by:

$$C = V_h + V_v + V_d \tag{16}$$

where V_h, V_v, and V_d represent the value of the expected cost associated with, respectively, hospitalization, intensive care, and death (for simplicity, we assume that symptoms are not associated with a cost unless one of these three events occurs).

Each of these cost components is itself the value of a probabilistic cost, as it depends on the cost of the generic event e (either, hospitalization, intubation, or death) and the probability of the occurrence of that event (conditional on having been infected), p^e. Therefore, it will be determined according to the equation:

$$V_e = \frac{C_e}{(1 + h\epsilon)^s} \tag{17}$$

with

$$\epsilon = \frac{1 - p^e}{p^e}$$

C_e is the cost of the generic event e (in case it happens). We set the cost of intubation equal to a multiple k of the cost of hospitalization and the cost of death as a multiple k of the cost of intubation (with k being a parameter greater than 1).

Agent subjective probabilities are determined by taking into account, sequentially:

• the publicly available information and

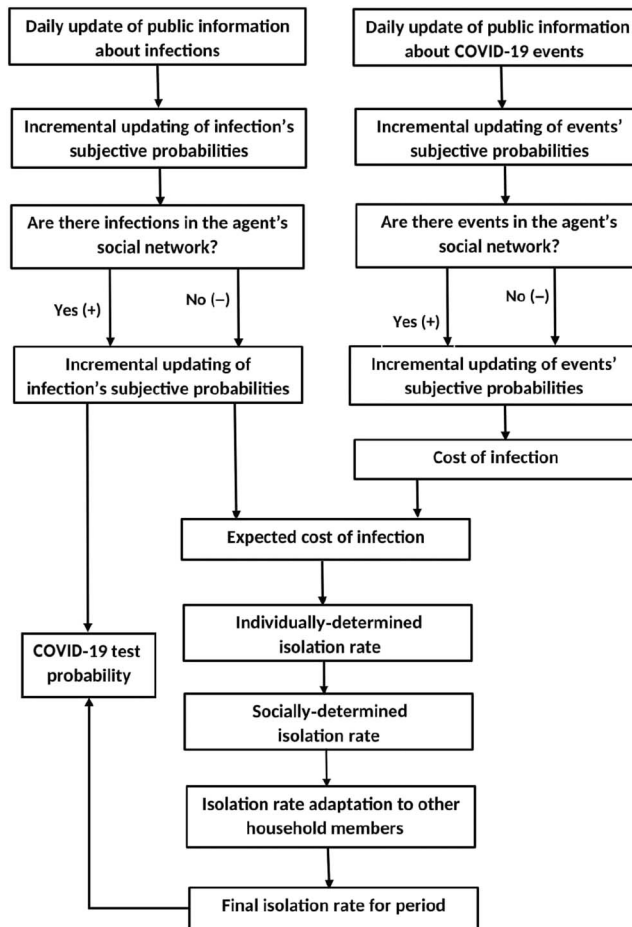• the direct observation of COVID-19 events (within the agent's social network)

Figure 3. Isolation and testing behaviour flowchart.

Then, with these probabilities, the expected cost of infection is calculated, and from this, the *individually-determined* isolation rate. The *final* isolation rate is the result of an incremental adjustment of this individually-determined isolation rate through the effect of the social pressure acting upon each agent, i.e., the individually-determined rates of the agents' social network and household members.

The flowchart of the behavioural determination of the agent isolation rate is shown in Figure 3.

2.3.2 Probabilities Estimation

In order to compute the expected cost of infection V, the relevant probabilities are the probability of infection, p^f; and, if infected, the probability of being hospitalized p^b, of being intubated p^v, and dying p^d.

From a normative point of view, decision theory dictates that when given alternative choices, individuals should select the alternative with the greatest expected benefit, given by the sum of the products between the probability of the choice's outcome and the value individuals attach to that outcome (Pratt et al., 1995). Harris et al. (2009), however, found experimental evidence that probabilities and outcomes are not independent: Severe events are usually associated with a higher occurrence probability than "neutral" events. Moreover, they showed that this relationship is mediated by the extent to which the occurrence of the event is controllable by the agents. W. F. Wright

and Bower's (1992) study, on the other hand, suggests a possible causal link between the severity of outcomes and the estimation of their probability, by showing that the subjective probability of events is affected by an individual's mood: Happy subjects overestimate the likelihood of positive events and underestimate that of negative events; sad subjects display the opposite tendencies, overestimating bad and underestimating good events. On the basis of these studies, we can argue that the higher the severity of a negative event, the stronger the effect of its occurrence will be on an individual's negative mood and, therefore, the stronger an agent's overestimation of the probability of its occurrence.

Taking stock of these empirical studies, we developed a model of the cognitive mechanism through which agents estimate the probabilities of the pandemic events (infection, hospitalization, intubation, and death). As for the three conditions (hospitalization, intubation, and death), we assume that the empirical probabilities of developing them by age group are publicly known, as they result from empirical studies. However, we assume that an agent's subjective perception of these probabilities diverges from the true (i.e., empirical) values, as agents process information from two other sources that they can observe in each period: the total number of events within an agent's age group, and the events an agent can directly observe within their household's social network. As for the former, the general idea is that agents adjust their subjective probability incrementally towards a value that is a biased measure of the empirical probability. Formally, the subjective probability of the event e in the current period, p_t^e, is given by:

$$p_t^e = p_{t-1}^e + \eta(p_w^e - p_{t-1}^e) \tag{18}$$

where η is a parameter of the model bounded between 0 and 1, determining how fast the subjective probability adapts to the new public information. In turn, the biased measure of the empirical probability, p_w^e, is given by:

$$p_w^e = p^* + (1 - p^*)(1 - e^{-\xi E}) \tag{19}$$

where p^* is the empirical, unbiased, probability of the event e, E is the number of new events in the agent's age group relatively to the agent's age group size, and ξ is a parameter of the model determining the strength of the bias, i.e., the agent's sensitivity to the public information regarding new cases (for $\xi = 0$, $p_w^e = p^*$; for $\xi \to \infty$, $p_w^e = 1$).

The second element affecting an agent's subjective probabilities is the information coming from their household's network. We assume that agents can observe the pandemic events (infection, hospitalization, intubation, and death) as they affect a member of a household belonging to their household's network. Following Epstein (2014), we model the effect of these events on probabilities by means of a simplified version of the Recorla-Wagner model (Recorla & Wagner, 1972): Each time an agent observes an event within their household's network, the probability of that event increases by a certain amount. Formally, being p_t^j the subjective probability before the event observation, the subjective probability after the observation of the event, $p_t^{e_o}$, is given by:

$$p_t^{e_o} = p_t^e + (1 - p_t^e)\frac{z_e}{q} \tag{20}$$

where q is a function of the geographical distance d between the town of the observing agent and the town of the observed agent (the assumption being that cases that are closer to the agent will have a higher effect on its subjective probabilities). Formally:

$$q = e^{\nu d} \tag{21}$$

As for z, it is a function of the difference between the agent's age and the age of the agent whose case has been observed. Calling g this difference, z is given by:

$$z_e = \frac{e^{\alpha_e g}}{e^{\alpha_e g} + 1} \tag{22}$$

where α_e is a parameter of the model. The value of z is bounded between 0, if the difference is a large negative number (i.e., the age of the agent whose case has been observed is much higher than the age of the observing agent), and 1, if the difference is a large positive number (i.e., the age of the agent whose case has been observed is much lower than the age of the observing agent). The assumption here is that the lower the age of the observed agent is compared to the age of the observing agent, the greater the effect will be on the subjective probability of the latter.

On the other hand, if in a certain period the agent does not observe any event, the probability for that event will decrease according to the equation:

$$p_t^{e_o} = p_t^e e^{-\rho} \tag{23}$$

where ρ represents the rate at which the occurrence probability of an event decreases as time goes by without the agent observing that event.

With regards to the probability of infection, the cognitive process is similar to the one described for the conditions. There are two important differences. First, differently from the probabilities of developing conditions, there is not an empirically established probability of infection, as it depends on a variety of factors besides the intrinsic infectiousness of the virus, such as the number of people who are around to pass the virus. While this probability cannot be but a very uncertain and subjective estimate, we can assume that it is somewhat associated with the virus' speed of circulation, approximated by the relative number of new infections in the agent's town (that is, the total infections in town divided by the town population). Formally, we define a speed of circulation index, f, defined by the equation:

$$f = 1 - e^{-\sigma E} \tag{24}$$

where E represents the relative number of infections in the agent's town. The speed of circulation index is bounded between 0, if $E = 0$, to a maximum (for $E = 1$), which depends on the parameter σ.

The subjective probability of infection for the period, p_t^f, is given by the marginal addition to the previous probability of infection of a fraction η of the difference between f and the previous probability of infection, where η is a parameter defining the probability's adjustment speed. Formally:

$$p_t^f = p_{t-1}^f + \eta(f - p_{t-1}^f) \tag{25}$$

The second difference concerns the weight through which the agent's subjective probability is updated after the observation of an event within the agent's social network (in this case, an infection) and, in particular, z: While before it was a function of the difference between ages, in this case it is a function of the difference between the observed agent isolation rate and the observing agent isolation rate δ_s. The assumption is that the greater the difference between the isolation rate of the infected agent and the isolation rate of the observing agent, the more the latter will revise its subjective probability of infection upwards. Formally:

$$z_f = \frac{e^{\alpha_f \delta_s}}{e^{\alpha_f \delta_s} + 1} \tag{26}$$

where α_f is a parameter of the model.

2.3.3 Self-Isolation Behaviour

This individually determined cost, V_i, determines both the *individual* self-isolation propensity, r_i and the agent's propensity to get tested for COVID-19.

Agents that do not take a test, or whose test result is negative, self-isolate with a certain probability s_i. The determination of the agent self-isolation rate, is a four-stage process. In the first stage, the agent individual *self-isolation propensity*, r_i, is determined through the equation:

$$r_i = 1 - e^{-\beta I_i V_i} \tag{27}$$

where I_i is the agent's income quintile (from 1, the poorest, to 5, the wealthiest), the assumption being that income has a positive effect on the agent's capacity and availability to self-isolate, while β is a parameter of the model. V_i is the value of the expected cost, determined in Equation 1. At this stage, we don't have the empirical data to validate the form of Equation 27: It has been chosen conveniently to ensure that the self-isolation propensity takes values starting from 0 (if at least one between income and expected cost if zero), and approaching 1 as income and expected cost increase. The income quintile appears in this equation because of the assumption, based on empirical evidence, that the likelihood of isolation increases with income level.

After the individual stage, in the second stage, the individual self-isolation attitude is affected by the social environment that agents are part of, for the effect of agent conformity to implicit social norms. First, we assume that the agent self-isolation behaviour is affected by the weighted average of the self-isolation propensities of the agent' friends, m_i. Formally:

$$m_i = \frac{\sum_{j=1}^{n} r_j e^{\theta d_{ij}}}{\sum_{j=1}^{n} e^{\theta d_{ij}}} \tag{28}$$

where n is the number of friends in the agent i's social network. The weight d_{ij} is the weight associated with the link between agent i and the agent's friend j, which is multiplied by a parameter θ. According to this equation, the stronger the link between an agent and a friend, the more weight the self-isolation propensity of this friend will have on the agent's self-isolation, with the parameter θ determining how fast this social influence decreases as the link's strength decreases.

Then, the socially affected self-isolation propensity r_i^n is equal to the individual self-isolation propensity, r_i, plus a share of the difference between r_i and the weighted social network mean self-isolation propensity, m_i. Formally:

$$r_i^n = r_i + \lambda(m_i - r_i) \tag{29}$$

where λ represents the agent sensitivity to social norms, a parameter that can take values between 1 (if agents conform perfectly to the mean self-isolation propensity of their friends) and 0 (if agents are not influenced by their friends).

Second, agent self-isolation propensity is adjusted at the *household* level. In particular, we assume, in line with empirical evidence, that households that can count on the help of other households, can more easily self-isolate, while the reverse is true for households that must care for other households. We assume that help is transferred between households linked by kin relationships. Formally, each household is associated with a *help availability index*, q_i, which is determined by the equation:

$$q_i = \frac{\sum_{j=1}^{n} A_{ij} e^{-\phi d_{ij}}}{\sum_{j=1}^{n} e^{-\phi d_{ij}}} \tag{30}$$

where n is the number of households with a kin relationship with household i and d_{ij} is the weight of household j's contribution, represented by the *kinship distance* between household i and the

related household j (weight that is multiplied by a parameter ϕ). A_{ij} is the difference between the mean ages of household i and household j. Therefore, households with a positive q_i (i.e., with a higher mean age than the average of the related households) will receive help and, therefore, adjust their mean self-isolation propensity upwards. Oppositely, households with a negative q_i (i.e., with a lower mean age than the average of the related households) will provide help and will adjust their mean self-isolation propensity downwards.

According to this equation, the more distant is the kinship relationship between two households, the smaller weight the help that could potentially be transferred between the two households will have on their self-isolation propensity, with the parameter ϕ determining how fast the influence of the potential help provision decreases as the kinship distance increases.

Formally, calling b_0 the mean isolation propensity of a household *before* the help provision, the household mean isolation propensity *after* the help provision, b, will be given by:

$$b = \begin{cases} b_0 + (r_{max} - b_0)(1 - e^{-\tau q_1}) & \text{if } q_i > 0 \\ b_0 - b_0(1 - e^{\tau q_1}) & \text{if } q_i < 0 \end{cases} \tag{31}$$

where r_{max} is the maximum individual self-isolation propensity within the household, which is the self-isolation propensity *unconstrained by income considerations*, given by Equation 11 setting the income quintile I_i to the highest level. The parameter τ represents the sensitivity of the household's mean self-isolation propensity to its help availability index.

Finally, individual self-isolation rate s_i is determined by adjusting the agent's self-isolation propensity r_i towards their household's mean propensity isolation, apart from members who tested positive to the virus, which maintain a complete self-isolation regime. Formally:

$$s_i = r_i + (b - r_i)\gamma \tag{32}$$

where b is the mean self-isolation propensity of agent i's household and γ is a parameter between 0 and 1.

The agent isolation rate is then used in the social interaction process to determine venue attendants. For each venue, after the pool of people who would normally attend is determined, each agent in the pool is removed with a probability equal to the agent's self-isolation rate. The parameters of the process determining the self-isolation rate are shown in Figure 4.

2.3.4 Testing Behaviour

In each period, agents take a test with a certain probability p_{test}, which is a function of the agent's social preferences μ (i.e., a measure of how much they care about not transmitting the virus to others, which is a random value drawn from the uniform distribution at their birth), the agent's income quintile I (the assumption being that agents will be more likely to take the test the more able they are to self-isolate after a positive result, an ability that is a positively related to their income level), and the agent's expected cost of infection, w. Formally:

$$p_{test} = 1 - e^{-\alpha^T \mu I w} \tag{33}$$

where α^T is a parameter of the model.

As for the agent's expected cost of infection, w, it is given by the product between the likelihood that the agent *has been* infected, p_f (please note that it is different from the probability of infection, p^f), and the value of the cost of being infected, V_i (determined in Equation 1). Formally:

$$w = p^f V_i \tag{34}$$

Parameter	Equation	Range	Default value
Expected cost of infection			
h	15–17	$[0, \infty]$	2
s	15–17	$[0, \infty]$	2
C_h	17	$[0, \infty]$	100
k	17	$[1, \infty]$	10
Probabilities (of events and infection)			
η	18–25	$[0, 1]$	0.2
ξ	19	$[0, \infty]$	60
ν	21	$[0, \infty]$	0.25
α_e	22	$[0, \infty]$	0.2
ρ	26	$[0, \infty]$	2
σ	23	$[0, 1]$	0.05
α_f	24	$[0, \infty]$	100
Individual isolation rate			
β	27	$[0, \infty]$	200
Social influence			
θ	28	$[0, \infty]$	1
λ	29	$[0, 1]$	0.25
φ	30	$[0, \infty]$	1
τ	31	$[0, \infty]$	0.02
γ	32	$[0, 1]$	0.5

Figure 4. Self-isolation rate parameters.

In turn, the likelihood that the agent has been infected, p^f depends on three variables: the severity of the agent's symptoms (if any); the presence in the household of an infected agent; the probability of having being exposed in a social setting, being a function of the agent's isolation rate s_i and of the agent's probability of infection, p_f, according to the following equation:

$$p^f = \frac{(N + H)S}{2} \tag{35}$$

where N represents the probability of having being infected during a social interaction, H the probability of having being infected through the agent's interactions with other members of its own household, and S is a factor taking values between 0 and 1, determined by the maximum value between a function of the agent's symptoms s, and the probability of being asymptomatic, p_a. Formally:

$$S = max(s^{\beta^T}, p_a) \tag{36}$$

where β^T is a parameter of the model. As for N, it is given by:

$$N = 1 - e^{-\gamma^T \rho^T} \tag{37}$$

where γ^T is a parameter of the model and ρ^T is the n-period mean (with n being the average duration of infection) of the product between agent isolation rate, s_i, and the subjective probability of infection, p_f, for each period in the last n periods. Finally, H is given by:

$$H = 1 - e^{-\lambda^T h^T} \tag{38}$$

Parameter	Equation	Range	Default value
α^T	33	$[0, \infty]$	100
β^T	36	$[0, \infty]$	1
γ^T	37	$[0, \infty]$	10
λ^T	38	$[0, \infty]$	0.5

Figure 5. Testing probability parameters.

where b^T represents the number of infected household members and λ^T is a parameter of the model. The parameters of the process determining the testing probability are shown in Figure 5.

For agents taking a test, the result can be positive if they have been infected or in the case of a false positive, or the result can be negative if they have not been infected or in the case of a false negative. In any case, if the test result is positive, they self-isolate completely, and take a new test after a fixed number of days that is a parameter of the model.

2.4 The Course of the Virus

The flowchart for the course of the virus is shown in Figure 6. Susceptible agents can become exposed through an exogenous process (for international travelers), or through interaction with other members of their household, or interaction with other agents they meet in their social activities.

Once an agent has become exposed, it is assigned one *infection course* over four possible courses: asymptomatic; symptomatic not hospitalized; hospitalized not in intensive care; in intensive care. In accordance with empirical studies, we assume that the probability of developing more serious conditions grows with age, decreases with social status, and is higher for males than for females (Abate et al., 2020; Brazeau et al., 2020; Ferguson et al., 2020; Guilmoto, 2020; Public Health of England, 2020; Verity et al., 2020; Yanez et al., 2020).
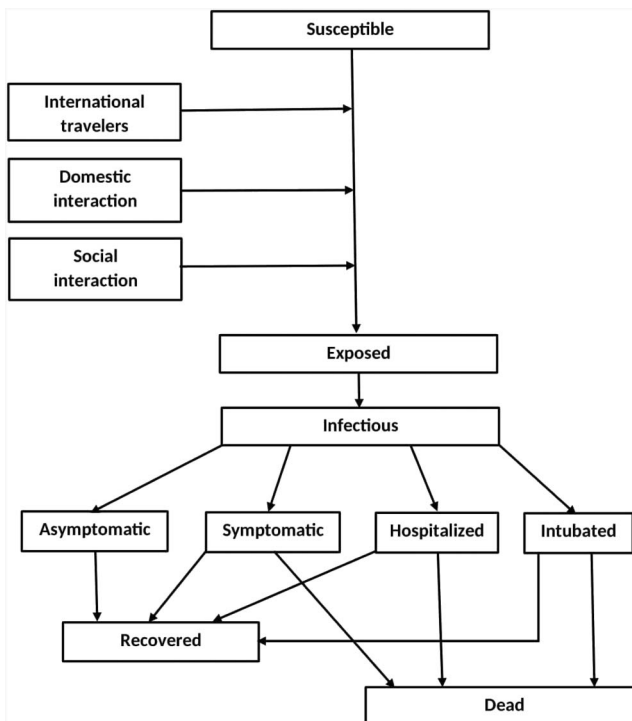
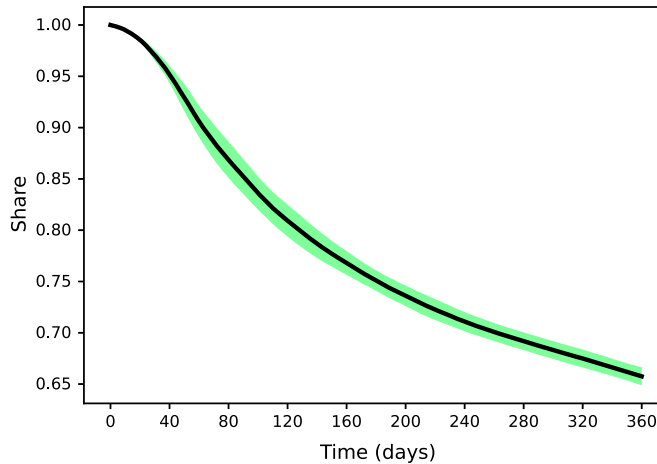Figure 6. Flowchart for the course of the virus.

Figure 7. Susceptible agents: share of population.

Upon exposure, the agent is also assigned an *incubation period*, which, in line with empirical observations (Lauer et al., 2020; McAloon et al., 2020), is drawn from a log-normal distribution with a mean of about 5 days, and a *recovery period*, whose length depends on the severity level assigned to the agent, in order to reproduce a log-normal distribution of the recovery period with a mean of about 12 days at the population level. The exposed agent is also assigned a *viral load*, which is drawn from a standard uniform distribution. The agent's viral load determines its contagiousness.

After the incubation period, the agent starts to develop symptoms (if not asymptomatic) and, in line with empirical observations (He et al., 2020), we assume that the exposed agent becomes infectious 2 days before the emergence of symptoms. The severity of symptoms of not-hospitalized symptomatic agents is differentiated by assigning them a *symptoms severity index*, between 0 and 1 exclusive, with the probability of the agent being assigned a higher value increasing with its viral load and its age, decreasing with its income quintile, and being higher for males than for females. The closer to 1 the symptoms severity index, the more severe the symptoms are, and the greater the reduction of the agent's mobility. Therefore, the agent's mobility is given by the minimum between the illness-affected mobility and the mobility resulting from the behaviourally determined isolation rate of its household. Finally, the agent's symptoms severity index determines the probability that the agent will take a test.

After the recovery period, a share of agents die, with a probability that also depends on age, social class, and gender. All other agents recover and we assume that they are immune to COVID-19 thereafter.

3   Simulation Results

In this section, we present the results of a benchmark simulation repeated 20 times (the black lines representing the average, and the green bands around it, the standard deviations).[2] In Figure 7 we show the share of susceptible agents in the population. Contrarily to the usual logistic curve of the traditional susceptible-exposed-infectious-recovered (SEIR) model, where the number of susceptible agents decreases quite fast in the central period of the pandemic, we can see here that the number of susceptible agents decreases quite slowly, with almost 65% of agents still susceptible after 360 days.

Correspondingly, the number of infections, shown in Figure 8, grows relatively quickly until its peak, after around 60 days, to slowly decrease thereafter.

---

2 The parameters used for the simulation are available in our GitHub repository at https://github.com/UmbertoGostoli/Pandemic
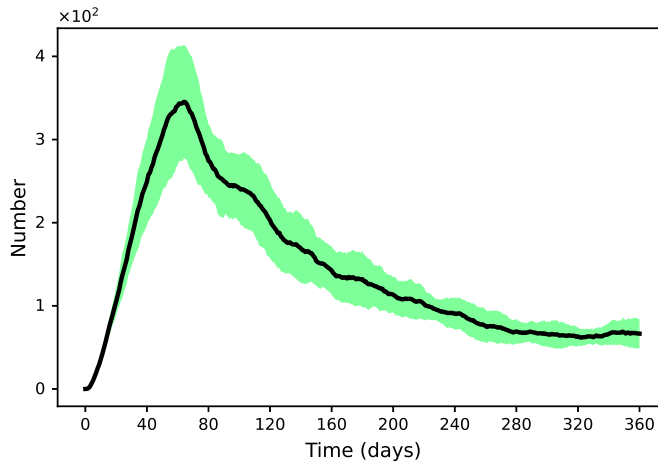   -Behaviour-Model/tree/Pandemic-Only-Sim.

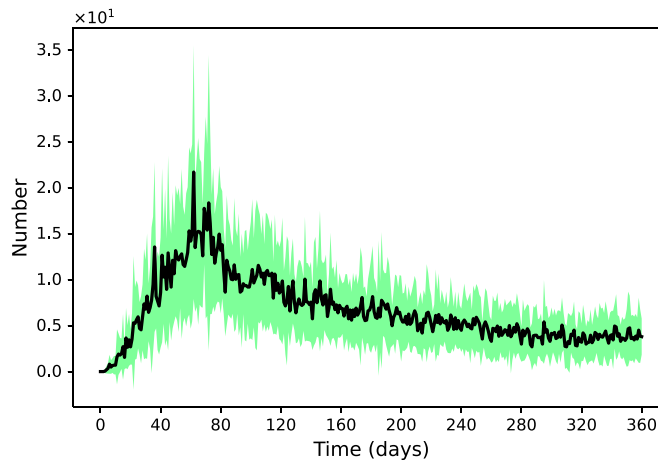Figure 8. Number of infectious agents.

Figure 9. Number of new cases.

A similar dynamics follows the number of new cases and hospitalizations, shown respectively in Figure 9 and Figure 10. The number of cases increases quite quickly to its peak after around 60 days, to decrease quite slowly from that point, through a series of irregular fluctuations.

Figure 11 shows the total attendances (i.e., the sum of all agents attending venues in a given day), whose dynamics is the result of the self-isolation generated by the behavioural model proposed in this article. We can see that agent self-isolation propensity increases up to the peak of the pandemic, where attendances are about 20% lower than the pre-pandemic figure. After the peak, attendances tend to recover but at a relatively slow pace, in line with the decrease of cases.

In the next three figures, we show how the pandemic has different outcomes depending on the agent's income quintile. Empirical studies have found conflicting evidence about the relationship between socioeconomic status and outcome severity. While some studies have found a positive relationship (Hawkins et al., 2020), other studies failed to find a clear relationship (Ingraham et al., 2021; Khan et al., 2021; Little et al., 2021). Our simulations confirm the complexity of the relationship between socioeconomic status and COVID-19 infections and outcomes. While the number of infections increases with the income quintiles (Figure 12), as we look at outcomes of increasing severity, the income quintiles that are most affected tend to move towards the lowest one: The
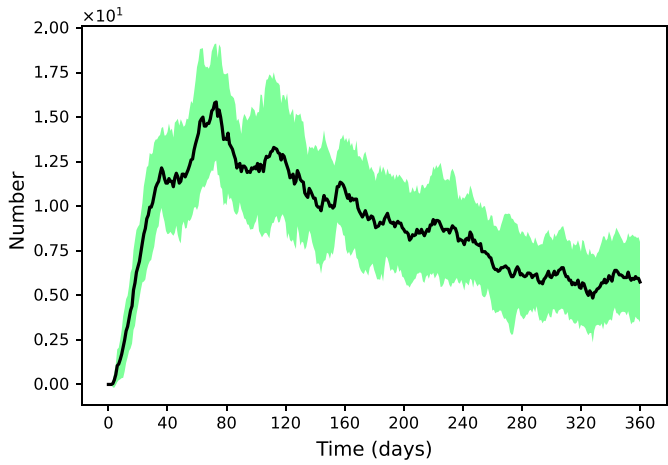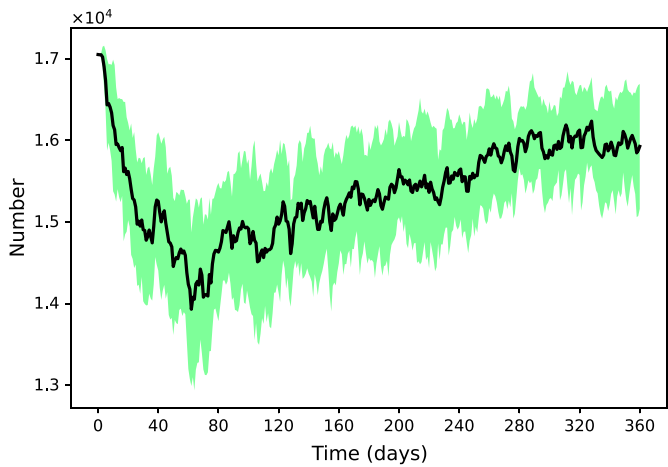
Figure 10. Number of hospitalized agents.

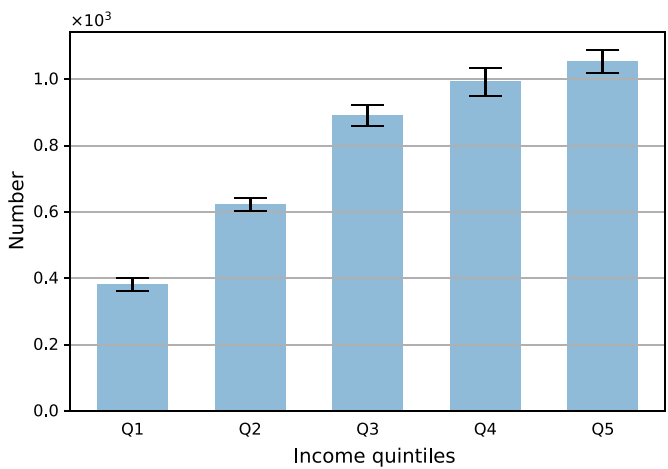Figure 11. Number of total attendances.

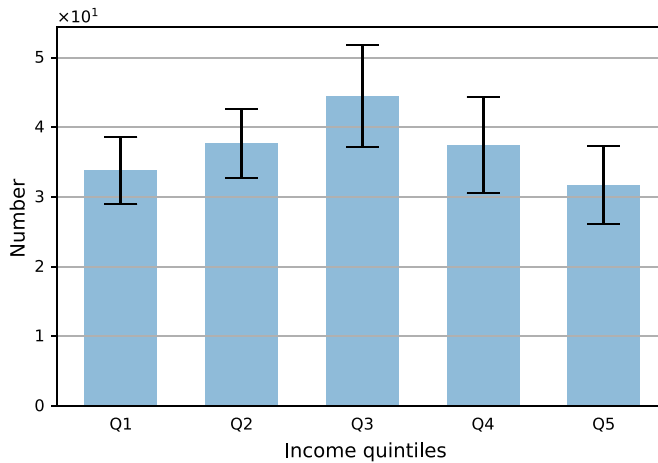
Figure 12. Total infections by income quintile.

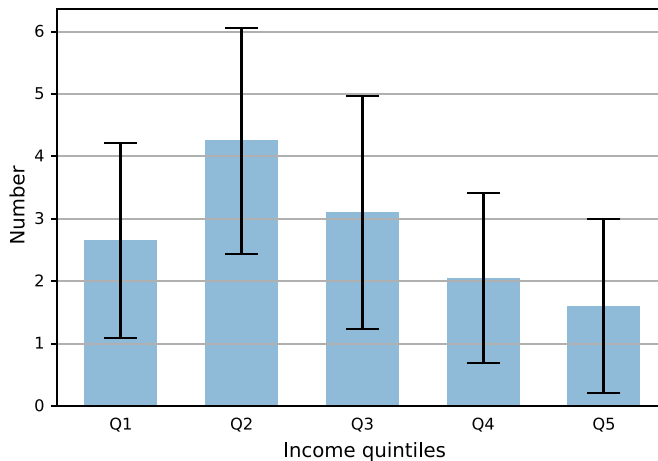Figure 13. Total hospitalizations by income quintile.

Figure 14. Total intubated by income quintile.

central quintiles are those with the highest number of hospitalizations (Figure 13) and the second quintile is that with the highest number of intubations (Figure 14). Note that in our model we do not consider the effect of comorbidity, which may account for a large part of the relationship between socioeconomic status and COVID-19 outcomes: These differences among income quintiles, therefore, are only the effect of the interaction among the different demographic structures, social interaction, and behavioural differences in the interaction patterns of agents belonging to different income levels.

Finally, Figure 15 shows the out-degree distribution of the infection network, where the degree represents the number of infected individuals by each contagious agent. We can see that the relationship between the frequency of degrees and the degrees on the log–log scale is approximately linear, (the R^2 being -0.97), with a scaling parameter of around 2.5, a typical value of scale-free networks. The fact that the model reproduces a scale-free infections network is rather surprising if we consider that from a behavioural point of view all the agents have a similar behaviour (apart from "linear" differences related to their age and socioeconomic status). Note that in the real world, the so called *super-spreaders*, are likely to infect more than 12–13 agents. However, we have to consider
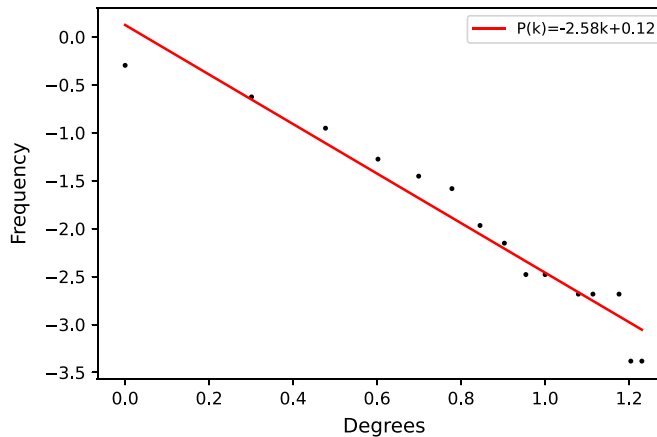
Figure 15. Degree distribution of the infection network. The *y* axis shows the log of the frequency of degrees (i.e., the log of the relative size of groups of spreaders, grouped by the number of people infected). The *x* axis shows the log of the degrees (i.e., the log of the number of people infected by a spreader, for each group).

that this result is highly dependent on the size of the population, which, because of computational constraints, we scaled down by a factor of 1 to 5,000.

3.1 Sensitivity Analysis

Finally, we conduct a sensitivity analysis to estimate the effect of a set of six parameters on the simulation's output. As the aim of this article is to introduce a behavioural model of self-isolation, the outcome we focus on is the total number of attendances during the pandemic: the lower this number, the higher the degree of self-isolation, on average. As for the choice of the parameters, we focused on six crucial processes of the complex behavioural model proposed, as described below:

- β, in Equation 27, determining the degree to which agent self-isolation propensity is sensitive to agent income level I and the value of the estimated cost V;

- σ, in Equation 24, determining the sensitivity of the agent's subjective estimate of the probability of infection to the relative number of new infections in the agent's town;

- ξ, in Equation 19, determining the effect of the relative number of new hospitalizations, intubations, and deaths on the agent's subjective estimate of the related probabilities;

- λ, in Equation 29, determining the effect of social norms on the agent self-isolation propensity;

- τ, in Equation 31, determining the effect of the availability of the kinship network's help on the household's mean self-isolation propensity; and

- ρ, in Equation 23, which is the fear of extinction rate.

From the sensitivity analysis we can see that within our theoretical framework, the parameter that most affects the degree of self-isolation is σ, the parameter determining the effect of the relative number of new infections in the agent's town on the agent's estimate of the probability of infection. (See Table 1.) The second most important parameter is β, determining the effect of the product between the income level and the value of the expected cost of infection V. We can notice that V depends on the probability of infection, whose value depends on σ. However, because of Equation 3, the leverage of σ happens to be greater than that of β. The third most important parameter is the fear of extinction rate.

Table 1. Sensitivity analysis.

Parameter	Equation	Range	Total effect
β	27	[20.0, 250.0]	30.26
σ	24	[20.0, 150.0]	59.19
ξ	19	[10.0, 100.0]	0.13
λ	29	[0.1, 0.5]	0.32
τ	31	[0.01, 0.05]	1.35
ρ	23	[0.01, 0.1]	10.17

On the other hand, the other three parameters have a much smaller effect. The most important parameter among these three is ν, which regulates the effect of a kinship network's help on a household's mean self-isolation, whereas the effect of the social norms and, especially, of the relative number of the various conditions (i.e., new hospitalizations, intubations, or deaths) is quite negligible. This last result is quite surprising if we consider that the relative number of new infections has the largest effect on the outcome. The reason is that public information is only one of the determinants of the subjective probabilities of events: These probabilities are also affected by the events that agents observe (or, do *not* observe) in each period within their household's network. Since the three events of hospitalization, intubation, and death are relatively rare for a large part of the population, the fear of extinction process is predominant over the effect of public information.

4 Conclusions

In this article we demonstrate a proof-of-concept model that simulates interactions among the behavioural adaptations of agents to the COVID-19 pandemic and the course of the pandemic itself. Our behavioural model allows households to reduce their social interactions due to their perceived risks of infection, which provides a first step towards the development of more policy-relevant agent-based models of COVID-19 and future pandemics. The results show that the propensity of agents to self-isolate in the presence of risk has a pronounced effect on the course of the pandemic, which is reflective of real-world outcomes.

We propose that this model can provide a basis for further exploration of behavioural responses to pandemics and their impact on disease transmission. The simulation also allows for the more detailed investigation of inequities in COVID-19 outcomes between different socioeconomic status groups. Future iterations of this model can examine additional health behaviours adopted in response to COVID-19, such as mask-wearing, social distancing, and vaccines, in order to further explore the behavioural responses to the wide variety of pharmaceutical and non-pharmaceutical interventions used during the pandemic.

Acknowledgments

References

Abate, S. M., Ahmed Ali, S., Mantfardo, B., & Basu, B. (2020). Rate of intensive care unit admission and outcomes among patients with coronavirus: A systematic review and meta-analysis. *PLOS ONE*, *15*(7), Article e0235653. https://doi.org/10.1371/journal.pone.0235653, PubMed: 32649661

Almagor, J., & Picascia, S. (2020). Exploring the effectiveness of a COVID-19 contact tracing app using an agent-based model. *Scientific Reports*, *10*(1), Article 22235. https://doi.org/10.1038/s41598-020-79000-y, PubMed: 33335125

Born, B., Dietrich, A. M., & Müller, G. J. (2021). The lockdown effect: A counterfactual for Sweden. *PLOS ONE*, *16*(4), Article e0249732. https://doi.org/10.1371/journal.pone.0249732, PubMed: 33831093

Brazeau, N., Verity, R., Jenks, S., Fu, H., Whittaker, C., Winskill, P., Dorigatti, I., Walker, P., Riley, S., Schnekenberg, R. P., Heltgebaum, H., Mellan, T., Mishra, S., Unwin, H., Watson, O., Cucunuba Perez, Z., Baguelin, M., Whittles, L., Bhatt, S., … Okell, L. (2020). *Report 34: COVID-19 infection fatality ratio: Estimates from seroprevalence*. Imperial College London. https://doi.org/10.25561/83545

Chattoe-Brown, E. (2021). Review of the book, *Social simulation for a crisis: Results and lessons from simulating the COVID-19 crisis*, Frank Dignum (Ed.). *Journal of Artificial Societies and Social Simulation*, *24*(4), 1. https://www.jasss.org/24/4/reviews/1.html

Dignum, F. (Ed.) (2021). *Social simulation for a crisis: Results and lessons from simulating the COVID-19 crisis*. Springer.

Epstein, J. M. (2014). *Agent_Zero: Toward neurocognitive foundations for generative social science*. Princeton University Press. https://doi.org/10.23943/princeton/9780691158884.001.0001

Epstein, J. M., Parker, J., Cummings, D., & Hammond, R. A. (2008). Coupled contagion dynamics of fear and disease: Mathematical and computational explorations. *PLOS ONE*, *3*(12), Article e3955. https://doi.org/10.1371/journal.pone.0003955, PubMed: 19079607

Ferguson, N., Laydon, D., Nedjati-Gilani, G., Imai, N., Ainslie, K., Baguelin, M., Bhatia, S., Boonyasiri, A., Cucunubá Perez, Z., Cuomo-Dannenburg, G., Dighe, A., Dorigatti, I., Fu, H., Gaythorpe, K., Green, W., Hamlet, A., Hinsley, W., Okell, L. C., van Elsland, S., … Ghani, A. C. (2020). *Report 9: Impact of non-pharmaceutical interventions (NPIs) to reduce COVID19 mortality and healthcare demand*. Imperial College London. https://doi.org/10.25561/77482

Gostoli, U., & Silverman, E. (2019). Modelling social care provision in an agent-based framework with kinship networks. *Royal Society Open Science*, *6*(7), Article 190029. https://doi.org/10.1098/rsos.190029, PubMed: 31417710

Gostoli, U., & Silverman, E. (2020). Social and child care provision in kinship networks: An agent-based model. *PLOS ONE*, *15*(12), Article e0242779. https://doi.org/10.1371/journal.pone.0242779, PubMed: 33264347

Green, L., Myerson, J., & Ostaszewski, P. (1999). Amount of reward has opposite effects on the discounting of delayed and probabilistic outcomes. *Journal of Experimental Psychology: Learning, Memory, and Cognition*, *25*(2), 418–427. https://doi.org/10.1037/0278-7393.25.2.418, PubMed: 10093208

Guilmoto, C. Z. (2020). *COVID-19 death rates by age and sex and the resulting mortality vulnerability of countries and regions in the world*. MedRxiv. https://doi.org/10.1101/2020.05.17.20097410

Harris, A. J. L., Corner, A., & Hahn, U. (2009). Estimating the probability of negative events. *Cognition*, *110*(1), 51–64. https://doi.org/10.1016/j.cognition.2008.10.006, PubMed: 19036359

Hawkins, R. B., Charles, E. J., & Mehaffey, J. H. (2020). Socio-economic status and COVID-19-related cases and fatalities. *Public Health*, *189*, 129–134. https://doi.org/10.1016/j.puhe.2020.09.016, PubMed: 33227595

He, X., Lau, E. H. Y., Wu, P., Deng, X., Wang, J., Hao, X., Lau, Y. C., Wong, J. Y., Guan, Y., Tan, X., Mo, X., Chen, Y., Liao, B., Chen, W., Hu, F., Zhang, Q., Zhong, M., Wu, Y., Zhao, L., … Leung, G. M. (2020). Temporal dynamics in viral shedding and transmissibility of COVID-19. *Nature Medicine*, *26*(5), 672–675. https://doi.org/10.1038/s41591-020-0869-5, PubMed: 32296168

Ingraham, N. E., Purcell, L. N., Karam, B. S., Dudley, R. A., Usher, M. G., Warlick, C. A., Allen, M. L., Melton, G. B., Charles, A., & Tignanelli, C. J. (2021). Racial and ethnic disparities in hospital admissions from COVID-19: Determining the impact of neighborhood deprivation and primary language. *Journal of General Internal Medicine*, *36*(11), 3462–3470. https://doi.org/10.1007/s11606-021-06790-w, PubMed: 34003427

Khan, K. S., Torpiano, G., McLellan, M., & Mahmud, S. (2021). The impact of socioeconomic status on 30-day mortality in hospitalized patients with COVID-19 infection. *Journal of Medical Virology*, 93(2), 995–1001. https://doi.org/10.1002/jmv.26371, PubMed: 32729937

Koehler, M., Slater, D. M., Jacyna, G., & Thompson, J. R. (2021). Modeling COVID-19 for lifting non-pharmaceutical interventions. *Journal of Artificial Societies and Social Simulation*, 24(2), Article 9. https://doi.org/10.18564/jasss.4585

Lauer, S. A., Grantz, K. H., Bi, Q., Jones, F. K., Zheng, Q., Meredith, H. R., Azman, A. S., Reich, N. G., & Lessler, J. (2020). The incubation period of coronavirus disease 2019 (COVID-19) from publicly reported confirmed cases: Estimation and application. *Annals of Internal Medicine*, 172(9), 577–582. https://doi.org/10.7326/M20-0504, PubMed: 32150748

Little, C., Alsen, M., Barlow, J., Naymagon, L., Tremblay, D., Genden, E., Trosman, S., Iavicoli, L., & van Gerwen, M. (2021). The impact of socioeconomic status on the clinical outcomes of COVID-19; a retrospective cohort study. *Journal of Community Health*, 46(4), 794–802. https://doi.org/10.1007/s10900-020-00944-3, PubMed: 33387149

McAloon, C., Collins, Á., Hunt, K., Barber, A., Byrne, A. W., Butler, F., Casey, M., Griffin, J., Lane, E., McEvoy, D., Wall, P., Green, M., O'Grady, L., & More, S. J. (2020). Incubation period of COVID-19: A rapid systematic review and meta-analysis of observational research. *BMJ Open*, 10(8), Article e039652. https://doi.org/10.1136/bmjopen-2020-039652, PubMed: 32801208

Noble, J., Silverman, E., Bijak, J., Rossiter, S., Evandrou, M., Bullock, S., Vlachantoni, A., & Falkingham, J. (2012). Linked lives: The utility of an agent-based approach to modeling partnership and household formation in the context of social care. In *Proceedings of the 2012 Winter simulation conference (WSC)* (pp. 1–12). ACM. https://doi.org/10.1109/WSC.2012.6465264

Pratt, J. W., Raiffa, H., & Schlaifer, R. (1995). *Introduction to statistical decision theory*. MIT Press.

Prem, K., Cook, A. R., & Jit, M. (2017). Projecting social contact matrices in 152 countries using contact surveys and demographic data. *PLOS Computational Biology*, 13(9), Article e1005697. https://doi.org/10.1371/journal.pcbi.1005697, PubMed: 28898249

Public Health of England. (2020). *Disparities in the risk and outcomes of COVID-19*. PHE Publications.

Pullano, G., Valdano, E., Scarpa, N., Rubrichi, S., & Colizza, V. (2020). Evaluating the effect of demographic factors, socioeconomic factors, and risk aversion on mobility during the COVID-19 epidemic in France under lockdown: A population-based study. *Lancet Digital Health*, 2(12), e638–e649. https://doi.org/10.1016/S2589-7500(20)30243-0, PubMed: 33163951

Rajabi, A., Mantzaris, A. V., Mutlu, E. C., & Garibay, O. O. (2021). Investigating dynamics of COVID-19 spread and containment with agent-based modeling. *Applied Sciences*, 11(12), Article 5367. https://doi.org/10.3390/app11125367

Rescorla, R. A., & Wagner, A. R. (1972). A theory of Pavlovian conditioning: Variations in the effectiveness of reinforcement and nonreinforcement. In A. H. Black, & W. F. Prokasy (Eds.), *Classical conditioning II: Current research and theory* (pp. 64–99). Appleton-Century-Crofts.

Shastry, V., Reeves, D. C., Willems, N., & Rai, V. (2022). Policy and behavioral response to shock events: An agent-based model of the effectiveness and equity of policy design features. *PLOS ONE*, 17(1), Article e0262172. https://doi.org/10.1371/journal.pone.0262172, PubMed: 35061776

Silva, P. C. L., Batista, P. V. C., Lima, H. S., Alves, M. A., Guimarães, F. G., & Silva, R. C. (2020). COVID-ABS: An agent-based model of COVID-19 epidemic to simulate health and economic effects of social distancing interventions. *Chaos, Solitons, and Fractals*, 139, Article 110088. https://doi.org/10.1016/j.chaos.2020.110088, PubMed: 32834624

Silverman, E. E., Hilton, J. J., & Bijak, J. J. (2013). Simulating the cost of social care in an ageing population. In W. Rekdalsbakken, R. T. Bye, & H. Zhang (Eds.), *EMCS 2013: Proceedings of the 27th European conference on modelling and simulation* (pp. 689–695). European Council for Modeling and Simulation. https://doi.org/10.7148/2013-0689

Smith, L. E., Amlôt, R., Lambert, H., Oliver, I., Robin, C., Yardley, L., & Rubin, G. J. (2020). Factors associated with adherence to self-isolation and lockdown measures in the UK: A cross-sectional survey. *Public Health*, 187, 41–52. https://doi.org/10.1016/j.puhe.2020.07.024, PubMed: 32898760

Verity, R., Okell, L. C., Dorigatti, I., Winskill, P., Whittaker, C., Imai, N., Cuomo-Dannenburg, G., Thompson, H., Walker, P. G., Fu, H., Dighe, A., Griffin, J. T., Baguelin, M., Bhatia, S., Boonyasiri, A., Cori, A., Cucunubá, Z., FitzJohn, R., Gaythorpe, K., ... Ferguson, N. M. (2020). Estimates of the severity

of coronavirus disease 2019: A model-based analysis. *Lancet Infectious Diseases*, *20*(6), 669–677. https://doi .org/10.1016/S1473-3099(20)30243-7, PubMed: 32240634

Wang, H., Paulson, K. R., Pease, S. A., Watson, S., Comfort, H., Zheng, P., Aravkin, A. Y., Bisignano, C., Barber, R. M., Alam, T., Fuller, J. E., May, E. A., Jones, D. P., Frisch, M. E., Abbafati, C., Adolph, C., Allorant, A., Amlag, J. O., Bang-Jensen, B., . . . Murray, C. J. L. (2022). Estimating excess mortality due to the COVID-19 pandemic: A systematic analysis of COVID-19-related mortality. *Lancet*, *399*(10334), 1513–1536. https://doi.org/10.1016/S0140-6736(21)02796-3, PubMed: 35279232

Wilder, B., Charpignon, M., Killian, J. A., Ou, H.-C., Mate, A., Jabbari, S., Perrault, A., Desai, A., Tambe, M., & Majumder, M. S. (2020). *The role of age distribution and family structure on COVID-19 dynamics: A preliminary modeling assessment for Hubei and Lombardy*. Available at https://crcs.seas.harvard.edu/files/covid_19_family _structure_8.pdf

Wright, A. L., Sonin, K., Driscoll, J., & Wilson, J. (2020). Poverty and economic dislocation reduce compliance with COVID-19 shelter-in-place protocols. *Journal of Economic Behavior & Organization*, *180*, 544–554. https://doi.org/10.1016/j.jebo.2020.10.008, PubMed: 33100443

Wright, W. F., & Bower, G. H. (1992). Mood effects on subjective probability assessment. *Organizational Behavior and Human Decision Processes*, *52*(2), 276–291. https://doi.org/10.1016/0749-5978(92)90039-A

Yanez, N. D., Weiss, N. S., Romand, J.-A., & Treggiari, M. M. (2020). COVID-19 mortality risk for older men and women. *BMC Public Health*, *20*(1), Article 1742. https://doi.org/10.1186/s12889-020-09826-8, PubMed: 33213391